Supporting Information

Hydrogen-induced defective crystalline carbon nitride with enhanced bi-directional charge migration for persulfate photoactivation

Huachun Lan, Qingwen Tang, Zhiang Hou, Kai Zhu, Xiaoqiang An*, Huijuan Liu, Jiuhui Qu

Center for Water and Ecology, State Key Joint Laboratory of Environment Simulation and Pollution Control, School of Environment, Tsinghua University, Beijing 100084, China

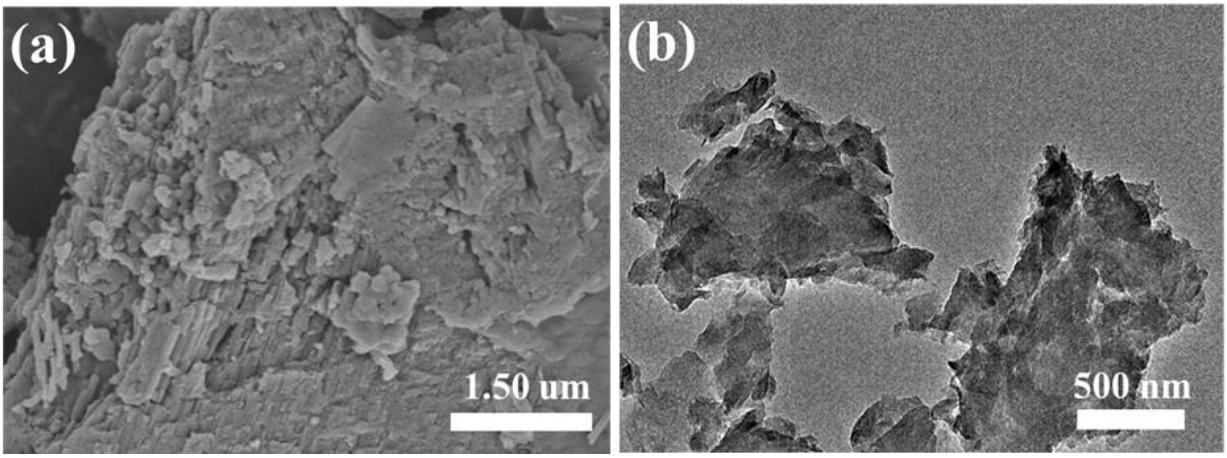

Figure S1. (a) SEM, (b) TEM image of g-C_3N_4.

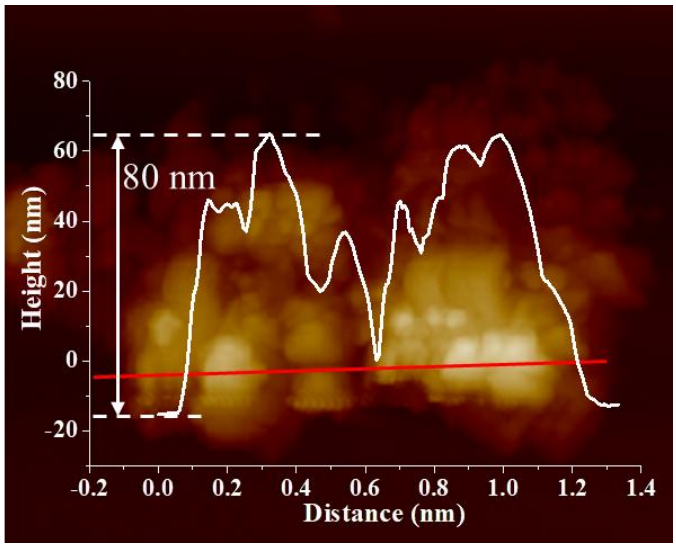

Figure S2. AFM image of g-C_3N_4.

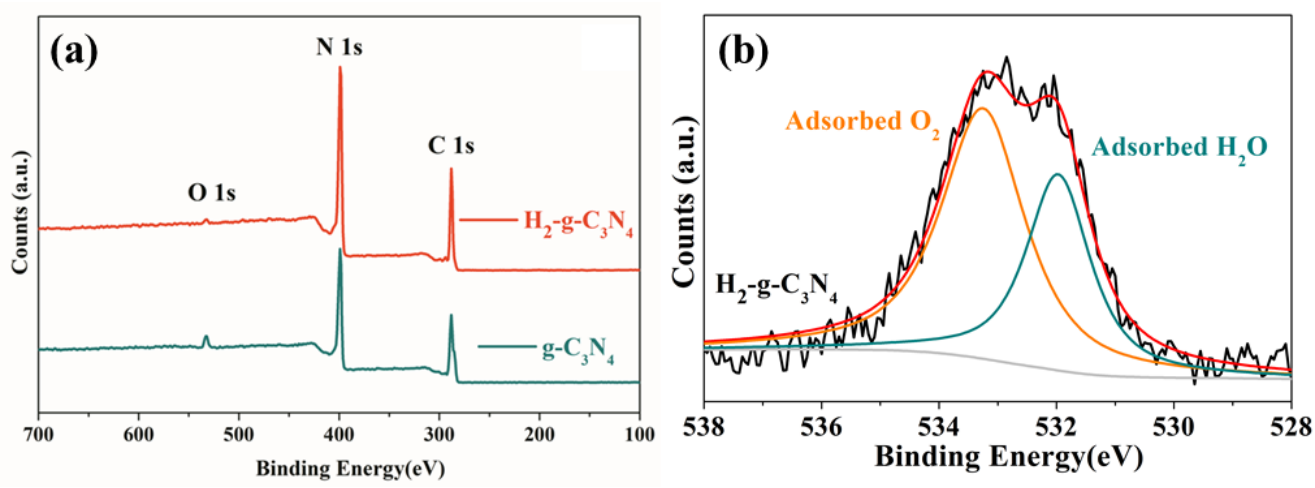

Figure S3. (a) XPS survey spectra for g-C_3N_4 and H_2-g-C_3N_4, (b) High resolution XPS spectrum of O1s in H_2-g-C_3N_4.

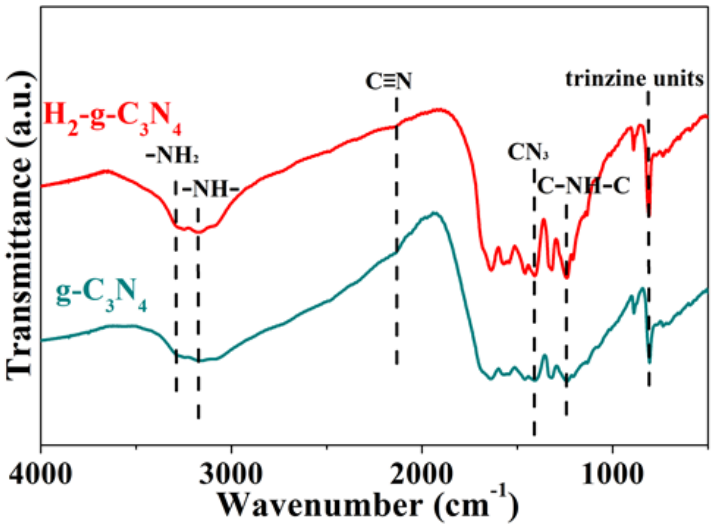

Figure S4. FTIR spectra of g-C_3N_4 and H_2-g-C_3N_4.

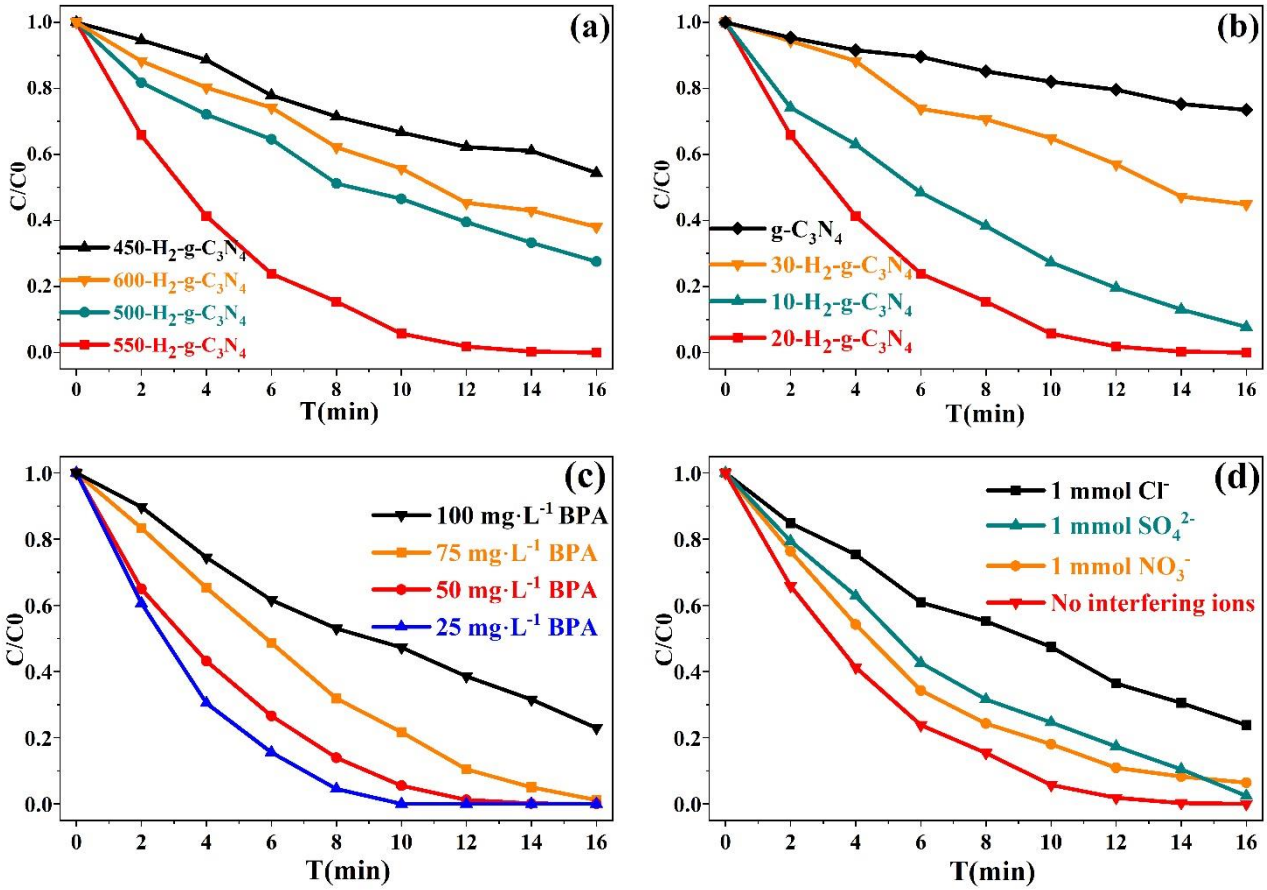

Figure S5. Effect of different calcination temperatures (a) and ventilation rate (b) on the efficiency of synergistic reactions. (c)The effect of BPA concentration and (d) inorganic anions on the synergistic degradation of BPA.

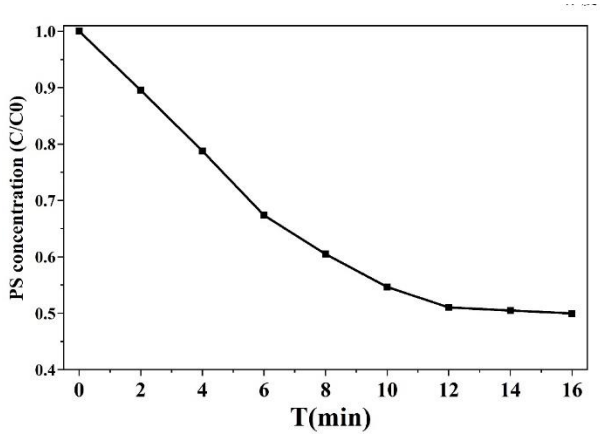

Figure S6. The change of persulfate concentration in the reaction solution as the reaction progresses.

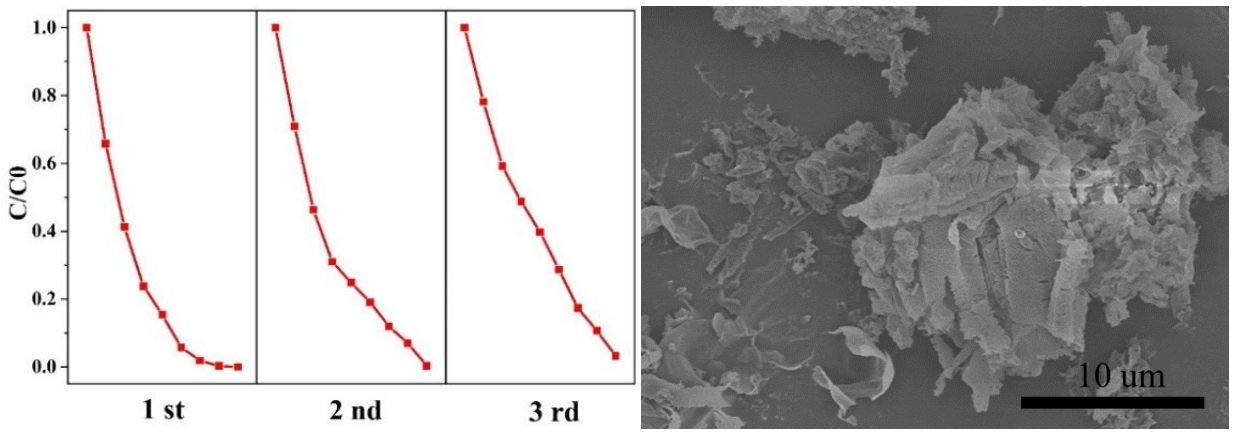

Figure S7. (a) Recycle tests of BPA degradation over H-g-C_3N_4 in the presence of persulfate and light irradiation. (b) SEM image of H-g-C_3N_4 after reactions.

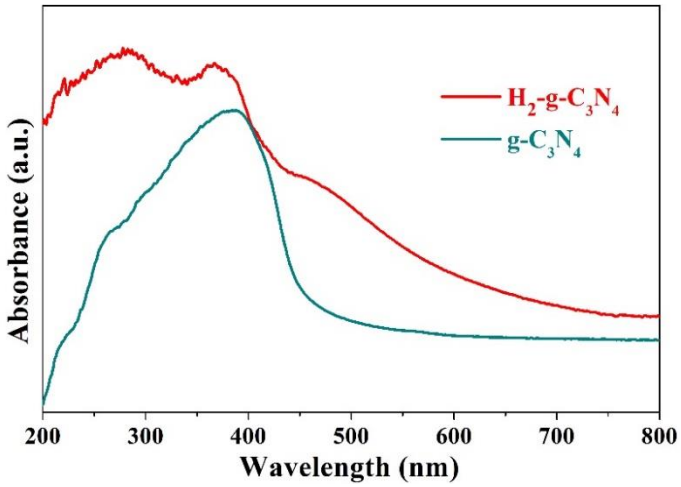

Figure S8. UV-vis diffuse reflectance spectra of g-C_3N_4 and H_2-g-C_3N_4.

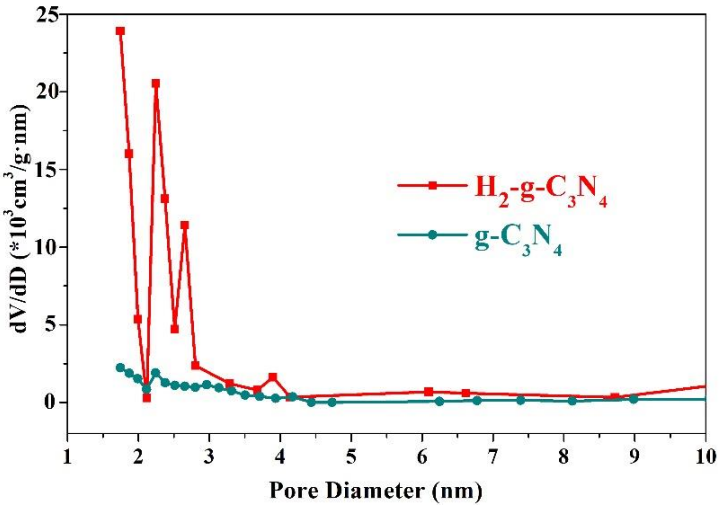

Figure S9. Pore size distribution curve of g-C_3N_4 and H_2-g-C_3N_4.

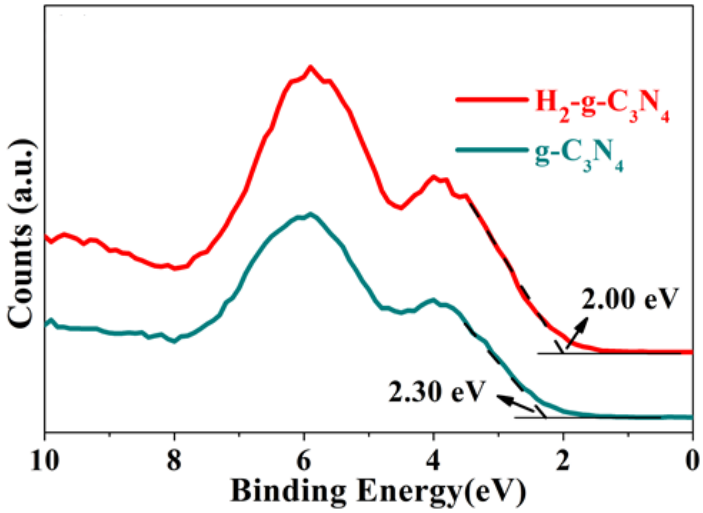

Figure S10. VB XPS spectra of g-C_3N_4 and H_2-g-C_3N_4.

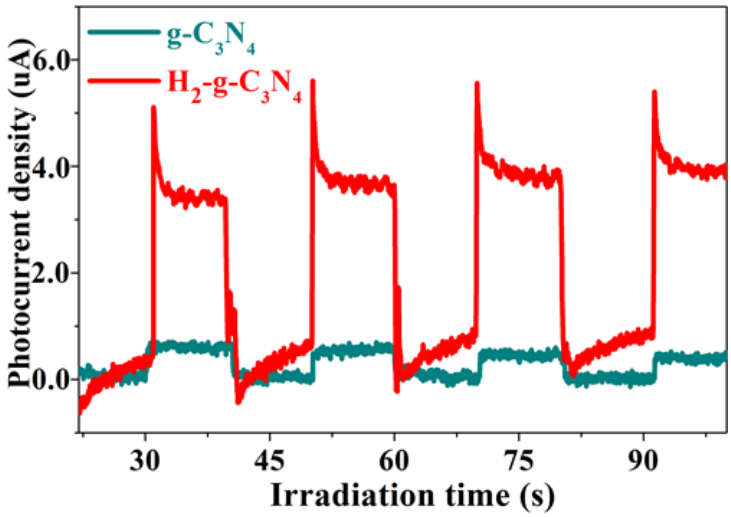

Figure S11. Photocurrent density curves of g-C_3N_4 and H_2-g-C_3N_4.

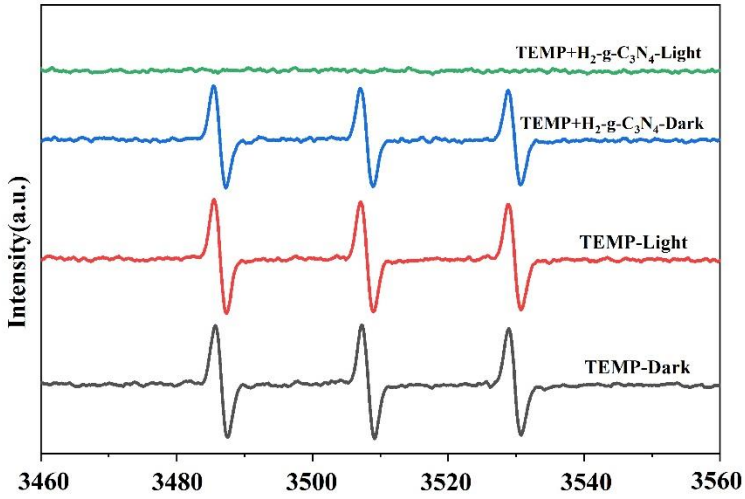

Figure S12. TEMP spin-trapping ESR spectra over H_2-g-C_3N_4 in different solvents.

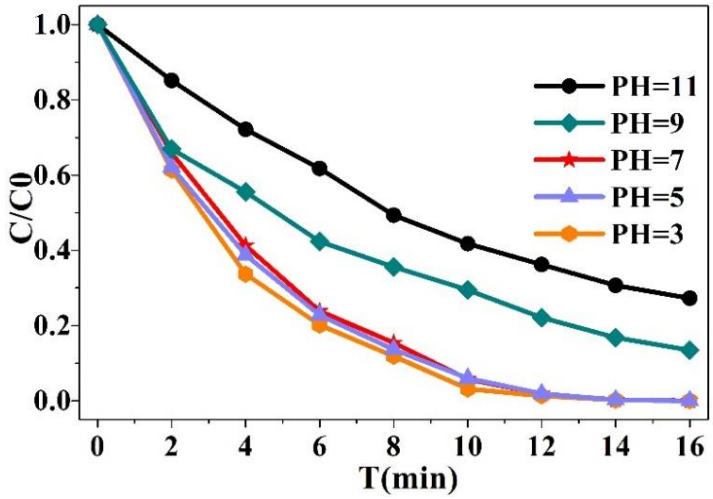

Figure S13. Degradation curves of BPA at different pH values over H_2-g-C_3N_4.

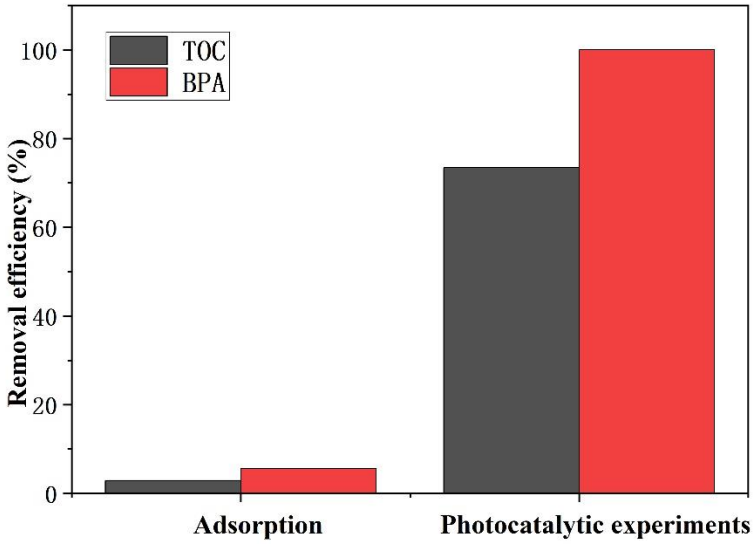

Figure S14. Pollutant removal efficiency by adsorption and photocatalytic.

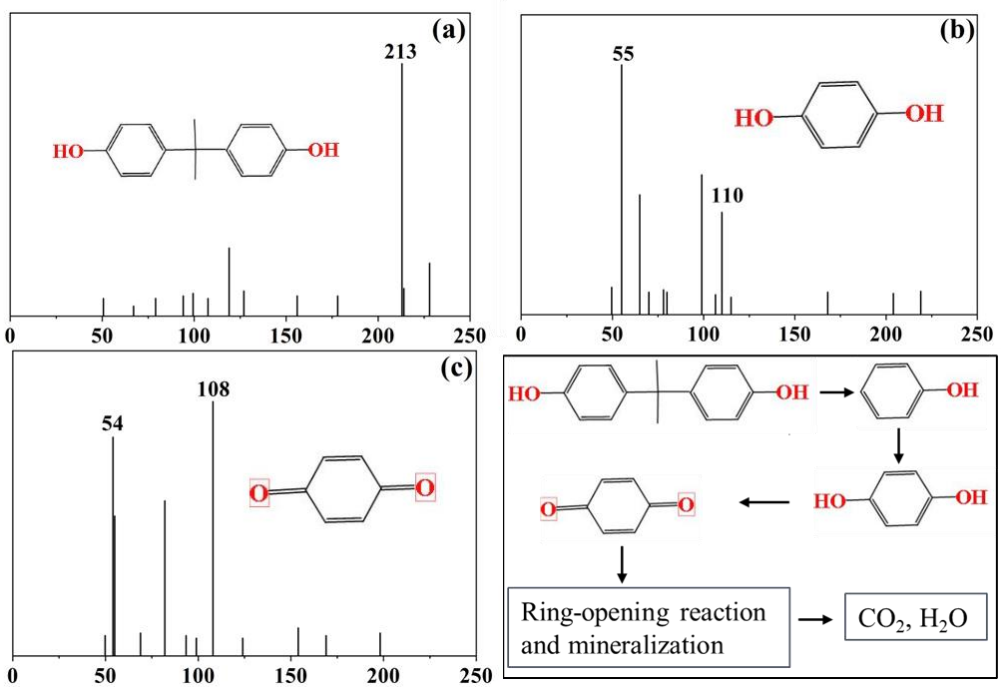

Figure S15. Proposed degradation pathway of BPA by H_2-g-C_3N_4+PS+Light system.

Table S1. The binding energy of two atomic layer of g-C_3N_4 and H_2-g-C_3N_4.

	E_{1L}	E_{2L}	ΔE_{bind}
g-C_3N_4	-12394.89	-24795.31	-5.52
H_2-g-C_3N_4	-12120.85	-24248.82	-7.11

Table S2. XPS survey spectra of g-C_3N_4 and H_2-g-C_3N_4.

Sample	XPS			C/N ratio	N-H	N-(C)3	C-N=C
	(C) %	(N) %	(O) %		%	%	%
g-C_3N_4	46.89	50.75	2.35	0.92	10.50	17.19	72.31
H_2-g-C_3N_4	49.48	43.01	6.75	1.15	22.35	30.42	47.23

Table S3. The comparison of performances of photocatalysts for BPA degradation efficiencies.

Catalyst	Light source	Catalyst Dosage (g/L)	PS/PMS Dosage (mM)	BPA Concentration (mg/L)	Complete Degradation time (time)	Rate constant (k, min^{-1})	Ref
BM200	300 W Xenon lamp	0.25	0.2	10	40	0.15	31
ECN60	300 W Xenon lamp (λ > 420 nm)	0.33	40.0	20	20	0.136	32
OVs-Zn_2SnO_4	300W Xe-arc lamp (λ >420 nm)	0.1	30.81	5	60	0.026	33
N,S:CQD/MIL-101(Fe)	350 W Xenon lamp (λ >400 nm)	0.4	3.0	20	60	0.0551	34
g-C_3N_4/MIL-101(Fe)	300 W Xenon lamp (λ >400 nm)	0.5	1.0	10	60	0.0589	35
Fe-POM/001-TiO_2	300 W Xenon lamp 200 mw/cm^2	0.5	1.85	50	25	0.195	36
BiOI/$Bi_2W_{0.25}Mo_{0.75}O_6$	300 W xenon lamp	1.0	1.5	15	30	0.06531	37
TGNF5@TOBC	300 W Xenon lamp (λ > 420 nm)	0.5	2.0	10	60	0.0522	38
CNBC	300 W Xenon lamp (λ > 420 nm)	1.0	1.0	5	60 (35%)	0.0559	39
Ag–Fe@BAB	250 W LED lamp (λ =400 nm)	1.0	0.5	10	80	0.056	40
g-C_3N_4-NS	150 W Xenon lamp (λ =400 nm)	0.5	5.0	5	60	0.0469	41
FeOOH@g-C_3N_4	300 W Xenon lamp (λ≥420 nm)	0.4	2.0	20	60	0.0568	42
PDI-P9	800 W Xenon lamp (λ > 420 nm)	0.5	1.5	5	15	0.248	43
SCF@GCN	low-pressure Hg UV-Clamp (λ = 240–260 nm)	0.3	4.0	20	15	0.34	44
MIL-88B	visible light 200 mw/cm^2	0.6	2.0	10	25	0.107	45
H_2-g-C_3N_4	300 W Xenon lamp 200 mw/cm^2	0.50	1.85	50	15	0.367	This Work

Table S4. BET surface areas and pore volumes of g-C_3N_4 and H_2-g-C_3N_4.

Sample	BET surface areas	pore volumes
	$m^2.g^{-1}$	$cm^3.g^{-1}$
g-C_3N_4	9.82	0.02
H_2-g-C_3N_4	65.56	0.14

Table S5. Lifetime Components of g-C_3N_4 and H_2-g-C_3N_4.

material	τ_1 (ns)	τ_2 (ns)	τ_3 (ns)	τ_{ave} (ns)
C_3N_4 (439nm)	1.87	6.207	45.37	9.48
H_2-g-C_3N_4 (439nm)	6.73	31.25	1.69	8.99